DTU Library

A model framework to describe growth-linked biodegradation of trace-level pesticides in the presence of coincidental carbon substrates and microbes

Liu, Li; Helbling, Damian E.; Kohler, Hans-Peter E.; Smets, Barth F.

[Link back to DTU Orbit](#)

A Model Framework to Describe Growth-Linked Biodegradation of Trace-Level Pollutants in the Presence of Coincidental Carbon Substrates and Microbes

Li Liu,[†] Damian E. Helbling,[‡,§] Hans-Peter E. Kohler,[‡] and Barth F. Smets*[,†]

[†]Department of Environmental Engineering, Technical, University of Denmark, Bygningstorvet 115, 2800 Kgs. Lyngby, Denmark

[‡]Eawag, Swiss Federal Institute of Aquatic Science and Technology, Department of Environmental Microbiology, Überlandstrasse 133, 8600 Dübendorf, Switzerland

[§]School of Civil and Environmental Engineering, Cornell University, Ithaca, New York 14850, United States

ABSTRACT: Pollutants such as pesticides and their degradation products occur ubiquitously in natural aquatic environments at trace concentrations (μg L^{-1} and lower). Microbial biodegradation processes have long been known to contribute to the attenuation of pesticides in contaminated environments. However, challenges remain in developing engineered remediation strategies for pesticide-contaminated environments because the fundamental processes that regulate growth-linked biodegradation of pesticides in natural environments remain poorly understood. In this research, we developed a model framework to describe growth-linked biodegradation of pesticides at trace concentrations. We used experimental data reported in the literature or novel simulations to explore three fundamental kinetic processes in isolation. We then combine these kinetic processes into a unified model framework. The three kinetic processes described were: the growth-linked biodegradation of micropollutant at environmentally relevant concentrations; the effect of coincidental assimilable organic carbon substrates; and the effect of coincidental microbes that compete for assimilable organic carbon substrates. We used Monod kinetic models to describe substrate utilization and microbial growth rates for specific pesticide and degrader pairs. We then extended the model to include terms for utilization of assimilable organic carbon substrates by the specific degrader and coincidental microbes, growth on assimilable organic carbon substrates by the specific degrader and coincidental microbes, and endogenous metabolism. The proposed model framework enables interpretation and description of a range of experimental observations on micropollutant biodegradation. The model provides a useful tool to identify environmental conditions with respect to the occurrence of assimilable organic carbon and coincidental microbes that may result in enhanced or reduced micropollutant biodegradation.
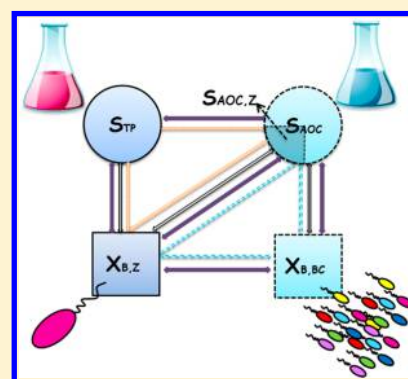
INTRODUCTION

Pesticides and other so-called micropollutants occur ubiquitously in natural aquatic environments[1,2] at trace concentrations typically in the low μg L^{-1} range and lower.[3] Microbial biodegradation processes have long been known to contribute to the natural attenuation of pesticides in contaminated environments. However, the fundamental processes that contribute to pesticide biodegradation are poorly understood. As a result, efforts to develop engineered biological remediation strategies have been limited.[1,4−6]

In this work, we consider three fundamental kinetic processes that could determine whether a pesticide is biodegraded in a natural environment. First, we consider the kinetics of pesticide utilization by a specific degrader strain. Many experimental approaches have been described to measure pesticide biodegradation kinetics at low concentrations.[7−11] Whereas some studies report shifts in biodegradation kinetics at low concentrations,[7−10] others have reported no shifts in kinetics down to the low μg L^{-1} range.[11] Nevertheless, biodegradation processes are generally considered to follow Monod kinetics

even at low concentrations.[11−13] Second, we consider the occurrence of coincidental organic carbon substrates. Most environments contain dissolved natural organic matter. The fraction of dissolved natural organic matter that can be utilized by microorganisms as a growth substrate is known as the assimilable organic carbon (AOC).[14−18] Some have observed positive kinetic effects of coincidental AOC on pesticide degradation,[19,20] others have observed negative kinetic effects,[21] and others still have observed no kinetic effects.[22,23] It is critical to understand the possible mechanisms by which coincidental carbon substrates effect the kinetics of growth-linked pesticide biodegradation processes. Third, we consider the occurrence of coincidental microbes. Coincidental microbes may compete with pesticide degraders for coincidental carbon substrates which could similarly effect the kinetics of growth-linked pesticide biodegradation.[20,24,25]

Studies on survival or die-off of pesticide degrader strains[26,27] have not explicitly considered the compounding effects of coincidental carbon substrates or coincidental microbes on the kinetics of pesticide biodegradation or the growth of the pesticide degrader strain. Several researchers have documented the ability of coincidental carbon to support the growth of specific pesticide degrading strains.[17,20,24] However, only a fraction of the coincidental carbon is typically accessible to the strains.[15] The uncertainty of how much of the coincidental carbon is available for the pesticide degrader makes it more complex to explain these experimental results. By using carefully controlled conditions, and mechanistically appropriate mathematical models, it might be possible to isolate and parametrize these various interactions, explain the variability in observed effects, and even predict scenarios that have not yet been experimentally tested. Vital et al.,[24] while studying survival of *Escherichia coli* in oligotrophic (i.e., low AOC concentrations) waters, made a first effort to describe the interaction between *E. coli* and coincidental microbes based on competition for AOC, which was parametrized in Monod-based growth and removal kinetics for both microbial partners. Their model assumed that a fraction of the AOC could be utilized by *E. coli*, while the coincidental microbes could utilize all of the AOC. However, this fraction was assumed to remain constant throughout the experiment, which resulted in poor model fits to the experimental data. The positive effect of coincidental carbon on trace-level pesticide degradation has also mathematically been explained by AOC supported growth of the degrader strains.[12,28] In other studies, it has been recognized that Monod-based growth kinetics may need to be supplemented with explicit consideration of endogenous metabolism kinetics when considering competition at low concentrations.[29]

To date no model has been proposed that can simultaneously capture the effect of low substrate concentrations, coincidental carbon, and the effect of coincidental microbes on the fate of micropollutant along with the vitality of the degraders. In this study, we introduce a general mathematical modeling framework to capture the phenomena associated with the biodegradation of pollutants present at trace concentrations (at or below $\mu g\ L^{-1}$ concentrations[11]) in a growth-dependent manner in oligotrophic aqueous environments. This model explicitly and additively considers the effects of coincidental carbon and coincidental microbes. The model framework is intentionally kept simple, by focusing on kinetics only and ignoring biochemical processes such as inhibition, induction, and catabolite repression. The kinetic phenomena that we considered are modeled as a suite of additive processes. Experimental results derived from the literature are used to illustrate how various components of the model behave and can be parametrized. Simulations with parametrized models are used to systematically explore the effects of competition for fractions of coincidental carbon and the effect of the presence or absence of coincidental microbes. The proposed model can be used as a tool to interpret experimental observations and to predict the outcome associated with the introduction of specific pesticide degraders in oligotrophic environments. This utility will contribute to evaluating scenarios in the development of engineered bio remediation strategies.

■ MATERIALS AND METHODS

The aim of this study is to develop and test a model framework to explore the conditions that affect the fate of a trace-level

pollutant (TP, at concentration S_{TP}) in a natural environment. The framework considers the presence of coincidental AOC (at concentration S_{AOC}) and coincidental microbes (background community, BC, at concentration $X_{B,BC}$). The assumptions are that the pollutant is biodegraded in a growth-dependent manner by a specific degrader strain (Z at concentration $X_{B,Z}$), but is not degraded by the coincidental microbes. Further, we assume that pollutant biodegradation is controlled by process kinetics and that biochemical mechanisms such as enzyme induction or inhibition are not important. Figure 1
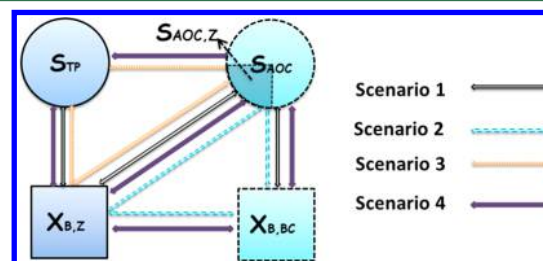

Figure 1. Possible interactions between trace-level pollutant (S_{TP}), coincidental carbon (S_{AOC}), pollutant degrader strains ($X_{B,Z}$) and coincidental microbes ($X_{B,BC}$) (arrows of same color refer to one scenario) in the full (4) and reduced scenarios (1−3).

provides the direct two-way interactions that were considered. The model is summarizedin the form of a Petersen Matrix,[30] which contains stoichiometric coefficients that describe how the state variables (columns) are affected by the different processes (rows) and rate expressions (last column) for each process (Table 1, with information on symbols, units and names in Table 2). Symbols for variables and parameters are named based on a standardized notation framework.[31]

The framework includes five state variables of which three are soluble carbon growth substrates (S_{TP}, $S_{AOC,Z}$ and $S_{AOC,other}$) and two are active biomass components ($X_{B,Z}$ and $X_{B,BC}$). We assume that other growth substrates (e.g., electron acceptors, N, P, etc.) are not limiting and that mass transfer processes are not relevant or fast. Hence, the framework is not sufficient to describe the biodegradation of compounds with low aqueous solubility in environmental matrices, where partitioning across different domains (e.g., gas, solid, liquid) would demand explicit inclusion of mass transfer kinetics.[32] Such processes could be added in extended models using established formulations.[33] Here, for the first time, we separate the coincidental carbon in two fractions: the fraction that can be utilized by the degrader strain ($X_{B,Z}$) termed $S_{AOC,Z}$, and the remaining fraction, termed $S_{AOC,other}$. Clearly the sum of $S_{AOC,Z}$ and $S_{AOC,other}$ remains S_{AOC}. Here we assume that the coincidental microbes have access to all of the S_{AOC}. We use parameter i ($i = (S_{AOC,Zo}/S_{AOCo})$) to express the initial fraction of coincidental carbon that can be utilized by the specific degrader strain.

Six microbial processes (P1−P6) are considered: (1) growth of degrader strain $X_{B,Z}$ coupled to removal of trace-level pollutant S_{TP}; (2) growth of degrader strain $X_{B,Z}$ coupled to removal of $S_{AOC,Z}$; (3) endogenous decay of degrader strain $X_{B,Z}$; (4) growth of coincidental microbes $X_{B,BC}$ coupled to consumption of $S_{AOC,Z}$; (5) growth of coincidental microbes $X_{B,BC}$ coupled to consumption of $S_{AOC,other}$; and (6) endogenous decay of coincidental microbes $X_{B,BC}$.

Simple models are proposed to describe growth kinetics, with only the concentration of the growth substrates themselves determining specific growth rate in a Monod-like saturation

Table 1. Matrix Notation of the Proposed Model Framework (V1–V5 are state variables, and P1–P6 are processes)

		V1	V2	V3	V4	V5	
		S_{TP}	$S_{AOC,Z}$	$S_{AOC,other}$	$X_{B,Z}$	$X_{B,BC}$	Kinetics Rates Expression
$X_{B,Z}$ (The Specific Degrader Strain)							
P1	growth $X_{B,Z}$ on S_{TP}	$-(1/Y_{TP,Z})$			1		$\mu_{XB,Z,TP,max} \dfrac{S_{TP}X_{B,Z}}{S_{TP} + K_{TP,Z}}$
P2	growth $X_{B,Z}$ on $S_{AOC,Z}$		$-(1/Y_{AOC,Z})$		1		$\mu_{XB,Z,AOC,max} \dfrac{S_{AOC,Z}X_{B,Z}}{S_{AOC,Z} + K_{AOC,Z}}$
P3	decay of $X_{B,Z}$				-1		$b_Z X_{B,z}$
$X_{B,BC}$ (Background Community)							
P4	growth $X_{B,BC}$ on $S_{AOC,Z}$		$-(1/Y_{AOCz,BC})$			1	$\mu_{XB,BC,AOCz,max} \dfrac{S_{AOC,Z}X_{B,BC}}{S_{AOC,Z} + K_{AOC,Z,BC}}$
P5	growth $X_{B,BC}$ on $S_{AOC,other}$			$-(1/Y_{AOCother,BC})$		1	$\mu_{XB,BC,AOcother,max} \dfrac{S_{AOC,other}X_{B,BC}}{S_{AOC,other} + K_{AOC,other,BC}}$
P6	decay of $X_{B,BC}$					-1	$b_{BC}X_{B,BC}$

dependency. This assumes no direct, neither positive nor negative, interactions between the removal of S_{TP} and S_{AOC}. We believe this assumption to be appropriate; although the biodegradation rates of anthropogenic chemicals can be inhibited by the presence of readily assimilable carbon sources through mechanisms such as catabolism repression,[34] such repression typically occurs at elevated concentrations of easily degradable substrates and AOC does not typically contain substrates supporting high growth rates.[14,35] Therefore, we ignore potential direct effects of coincidental carbon on removal of S_{TP}. In addition, while it is known that many anthropogenic chemicals may have growth inhibitory effects, these effects are again noted at elevated concentrations: given our specific interest in describing the fate of these chemicals at trace concentrations, we can again safely ignore potential direct negative effects of S_{TP} on growth of either $X_{B,Z}$ or $X_{B,BC}$. Endogenous metabolism is included using the formalism of continuous biomass decay, assumed as having a first-order dependence on the actual biomass concentration.

The ultimate goal is to use the model framework to capture scenarios that consider all 5 state variables and 6 processes. In addition, three reduced scenarios versus full Scenario 4 (considering all processes) can be identified to isolate one or few processes (Figure 1). These scenarios are useful constructs, as they allow us to test the validity of the proposed approach to model the interactions, and can also serve as tools to help parametrize submodel components, as parameter identification may become ill-posed with all processes occurring simultaneously.

As a result, the dynamics of the specific pollutant degrading strain's density can be described as follows:

$$\frac{dX_{B,Z}}{dt} = \mu_{XB,Z,TP,max} \underbrace{\frac{S_{TP}X_{B,Z}}{S_{TP} + K_{TP,Z}}}_{growth\ on\ S_{TP}} + \mu_{XB,Z,AOC,max} \underbrace{\frac{S_{AOC,Z}X_{B,Z}}{S_{AOC,Z} + K_{AOC,Z}}}_{growth\ on\ S_{AOC,Z}} - b_Z \cdot X_{B,Z} \tag{1}$$

And the dynamics of the coincidental microbial density is as follows:

$$\frac{dX_{B,BC}}{dt} = \mu_{XB,BC,AOCz,max} \underbrace{\frac{S_{AOC,Z}X_{B,BC}}{S_{AOC,Z} + K_{AOC,Z,BC}}}_{growth\ on\ S_{AOC,Z}} + \mu_{XB,BC,AOCother,max} \underbrace{\frac{S_{AOC,other}X_{B,BC}}{S_{AOC,other} + K_{AOC,other,BC}}}_{growth\ on\ S_{AOC,other}} - b_{BC}X_{B,BC} \tag{2}$$

In Scenario 1 only one growth substrate and one degrader are present. These experiments are ideal to estimate microbial growth and substrate utilization kinetic parameters (K_s and μ_{max}). Experimentally, this would mean the presence of the specific degrader strain with either the target pollutant or AOC present, or the coincidental microbes with AOC present. Equations 1 and 2 would then reduce to eq 3, while the dynamics of the growth substrate would follow eq 4:

$$\frac{dX}{dt} = \frac{\mu_{max}S}{K_s + S}X \tag{3}$$

$$\frac{dS}{dt} = -\frac{1}{Y}\frac{\mu_{max}S}{K_s + S}X \tag{4}$$

In addition, Y [cells substrate^{-1}] can be inferred from such experiments from a mass balance on cell density and substrate concentration. While concerns have been raised about how to conduct such experiments to make sure the kinetics are truly predictive of growth and substrate removal at trace levels,[7−10] Helbling et al.[11] has described a comprehensive methodology to execute those experiments for trace-level pesticide growth and utilization kinetics, and revealed that, with appropriate removal of coincidental carbon, growth kinetics obtained at higher concentrations are adequate descriptors of growth and substrate removal at trace concentrations for two unique substrate-degrader pairs. Also, growth on coincidental carbon, either by specific degraders as well as mixed coincidental microbes, can be adequately described using Monod growth kinetics.[24] Hence, we argue that sufficient experimental support exists that the two-way interactions between growth substrate and microbial types can be adequately described by Monod growth kinetics, and that experimental approaches exist to estimate the relevant parameters.[24]

Scenario 2 involves the presence of both a specific degrader strain and coincidental microbes, both growing and competing on coincidental carbon. Those experiments have rarely been performed, as a proper analysis requires that the specific strain can be selectively enumerated. Nevertheless, in some studies (e.g., Tarao et al.[20] and Vital et al.[24]) precisely such data was

Table 2. Initial Condition, Kinetic and Stoichiometric Parameters for Different Cases in Each Scenario

parameter	definition	case 1 (Figure 2) value	units	source	case 2 (Figure 4) value	units	source	case 3 (Figure 3 and 5) value	units	source
$Y_{AOCz,BC}$	yield of $X_{B,BC}$ on $S_{AOC,Z}$	11 000	cells (μg consumed substrate)$^{-1}$	(1)	1×10^{6}	CFU (μg C)$^{-1}$	(3)	1×10^{6}	cells (μg substrate)$^{-1}$	(2)
$Y_{AOCother,BC}$	yield of $X_{B,BC}$ on $S_{AOC, other}$	11 000	cells (μg consumed substrate)$^{-1}$	(2)	1×10^{6}	CFU (μg C)$^{-1}$	(2)	1×10^{6}	cells (μg substrate)$^{-1}$	(2)
Y_{AOCZ}	yield of $X_{B,Z}$ on S_{AOC}	5720	cells (μg consumed substrate)$^{-1}$	(1)	1×10^{6}	CFU (μg C)$^{-1}$	(3)	1×10^{6}	cells (μg substrate)$^{-1}$	(2)
$Y_{TP,Z}$	yield of $X_{B,Z}$ on S_{TP}				1×10^{6}	CFU (μg C)$^{-1}$	(3)	1×10^{6}	cells (μg substrate)$^{-1}$	(2)
i	the amount of coincidental carbon available for $X_{B,Z}$	0.53		(1)	0.1		(3)	0.5		(2)
b_{BC}	first order decay rate coefficient of $X_{B,BC}$	0.001	h^{-1}	(2)	0.001	d^{-1}	(2)	0.001	h^{-1}	(2)
b_Z	first order decay rate coefficient of $X_{B,Z}$	0.001	h^{-1}	(2)	0.001	d^{-1}	(2)	0.001	h^{-1}	(2)
$K_{AOC,Z}$	half-saturation coefficient of $X_{B,Z}$ on $S_{AOC,Z}$	489	μg L^{-1}	(1)	25.0	μg C mL^{-1}	(4)	500	μg L^{-1}	(2)
$K_{TP,Z}$	half-saturation coefficient of $X_{B,Z}$ on S_{TP}				1.76	μg C mL^{-1}	(4)	100	μg L^{-1}	(2)
$K_{AOCz,BC}$	half-saturation coefficient of $X_{B,BC}$ on $S_{AOC,Z}$	7.4	μg L^{-1}	(1)	991.77	μg C mL^{-1}	(4)	50	μg L^{-1}	(2)
$K_{AOC,other,BC}$	half-saturation coefficient of $X_{B,BC}$ on $S_{AOC,other}$	8.0	μg L^{-1}	(2)	700.0	μg C mL^{-1}	(2)	50	μg L^{-1}	(2)
$\mu_{XB,BC,AOCz,max}$	maximum specific rate of growth of $X_{B,BC}$ on $S_{AOC,Z}$	0.329	h^{-1}	(1)	843.71	d^{-1}	(4)	5	mg substrate (mg cells)$^{-1}$h^{-1}	(2)
$\mu_{XB,BC,AOCother,max}$	maximum specific rate of growth of $X_{B,BC}$ on $S_{AOC,other}$	0.134	h^{-1}	(2)	10.0	d^{-1}	(2)	5	mg substrate (mg cells)$^{-1}$h^{-1}	(2)
$\mu_{XB,Z,BC,AOC,max}$	maximum specific rate of growth of $X_{B,Z}$ on S_{AOC}	0.873	h^{-1}	(1)	6.29	d^{-1}	(4)	0.5	mg substrate (mg cells)$^{-1}$h^{-1}	(2)
$\mu_{XB,Z,TP,max}$	maximum specific rate of growth of $X_{B,Z}$ on S_{TP}				7.05	d^{-1}	(4)	5	mg substrate (mg cells)$^{-1}$h^{-1}	(2)
S_{AOC0}	initial concentration of the coincidental carbon	911	μg L^{-1}	(1)	7	μg C mL^{-1}	(3)	10–1000	μg L^{-1}	(2)
$S_{AOC,Z0}$	initial concentration of the coincidental carbon that can be utilized by $X_{B,Z}$	486.5	μg L^{-1}	(1)	0.7	μg C mL^{-1}	(3)	5–500	μg L^{-1}	(2)
$S_{AOC,other0}$	initial concentration of the coincidental carbon that cannot be utilized by $X_{B,Z}$	424.5	μg L^{-1}	(1)	6.3	μg C mL^{-1}	(3)	5–500	μg L^{-1}	(2)
S_{TP0}	initial concentration of the trace-level pesticide				1.0	μg C mL^{-1}	(3)	1000	μg L^{-1}	(2)
$X_{B,Z0}$	initial concentration of the specific trace-level pesticide degrader strain	700	cells L^{-1}	(1)	100	CFU mL^{-1}	(3)	1000	cell L^{-1}	(2)
$X_{B,BC0}$	initial concentration of the coincidental microbes in the coincidental carbon environment	8000	cells L^{-1}	(1)	1000	CFU mL^{-1}	(3)	1000	cell L^{-1}	(2)

Source: (1) Vital et al.;[24] (2) assumed in this study; (3) Tarao et al.;[20] (4) estimated.

obtained. Such data can then be used to assess whether the interaction between $X_{B,Z}$ and $X_{B,BC}$ is indeed the indirect effect of competition for coincidental carbon—as assumed in the proposed model—rather than the result of any direct positive or negative interactions.

Scenario 3 considers pesticide degradation at trace levels, by specific degrader strains, in the presence of coincidental carbon but in the absence of any coincidental microbes. These experiments have not typically been performed in a careful manner, although we contend that many biodegradation experiments—in practice—are of this type due to the incomplete removal of coincidental carbon in typical laboratory setups.[36,37] Such experiments are essential to verify that indeed no direct interaction between S_{TP} and S_{AOC} needs to be considered. Assuming this to be true, we can then examine how different initial concentrations of S_{TP} versus S_{AOC}; different accessibility to coincidental carbon by the specific degrader strains (i from 0 to 1); or different relative kinetics for S_{TP} vs $S_{AOC,Z}$, removal by the specific degrader would affect the fate of the trace-level pollutant.

Scenario 4 would then consider all five state variables, and all possible interactions, captured in all six processes. While Scenario 4 is the realistic scenario for most engineered bioremediation efforts, adequate monitoring of such scenarios for model calibration purposes would require the simultaneous measurement of all five (or at least four, as only total coincidental carbon is typically measurable) state variables. Such data is typically absent, and a thorough assessment of the simple additive approach to model this scenario is not yet feasible. Nevertheless, in silico predictions based on scenarios of reduced complexity can be made to test the ability of this model against some published experimental data.[20,24] With such preliminary confirmation of the validity of the approach, comprehensive simulations can then be performed to test the effect of different initial S_{AOC}, S_{TP} concentrations on S_{TP} fate.

To compare observed removal rates under varying scenarios, we define a reference removal rate as the inverse of the time required to remove 99% of the pollutant (eq 5). Changes in removal rates, due to the presence of coincidental carbon, are then expressed with respect to this reference removal rate by R (eq 6):

$$S_{TP} \text{ removal rate } (h^{-1}) = \frac{1}{\text{time used for 99\% removal of } S_{TP}}$$
(5)

$$R = \frac{S_{TP} \text{ removal rate } (h^{-1}) \text{ in presence of } S_{AOC}}{S_{TP} \text{ removal rate } (h^{-1}) \text{ in absence of } S_{AOC}}$$
(6)

AQUASIM 2.1 was used to code the presented model equations, using the mixed reactor compartment module to present fully mixed batch reactor conditions. Models were fit to published experimental data describing various reduced scenarios and parameters were estimated by minimizing the sum of the squared residuals. The standard deviation for parameter estimation defined globally for all data points was set to 10% to ensure the validity of the obtained parameter values.

RESULTS AND DISCUSSION

Initial conditions and best-fit parameter values for all experimental scenarios discussed below are summarized in Table 2.

Single Substrate, Single Microbe(s). Scenario 1 considers growth-linked removal of a single substrate by a single

microbial type (either strain or community). We contend that sufficient support exists for using Monod-like equations to describe growth-linked removal of pesticides at trace levels, as well as growth-linked removal of coincidental carbon, both by pesticide degrader strains and by coincidental microbes.[11−13] However, we wish to emphasize that proper estimation of the relevant model biokinetic and stoichiometric parameters requires careful experimental design. Ideally, processes are measured at environmentally relevant concentrations and under conditions that restrict the occurrence of coincidental carbon and coincidental microbes. Therefore, we will not directly probe Scenario 1 in this manuscript Rather, we will assume from these earlier reports that sufficient basis exists for kinetic description of Scenario 1, which can serve as a component in the additive model formulation.

Single Substrate, Mixed Microbes. Scenario 2 considers the competition between pesticide degrader strains and coincidental microbes for coincidental carbon (AOC) sources. Here, we analyzed an experiment that monitored the growth of a specific strain on coincidental carbon in the presence and absence of coincidental microbes. We used the experimental data from Vital et al.[24] to test the predictive abilities of the model. In this example, the pathogen *E. coli* O157 was grown in competition with drinking water coincidental microbes (X_{BC}) on natural coincidental carbon originating from diluted wastewater. The raw data derived from the published experiments and the results of our model simulations are presented in Figure 2. Vital et al.[24] also estimated the individual kinetic
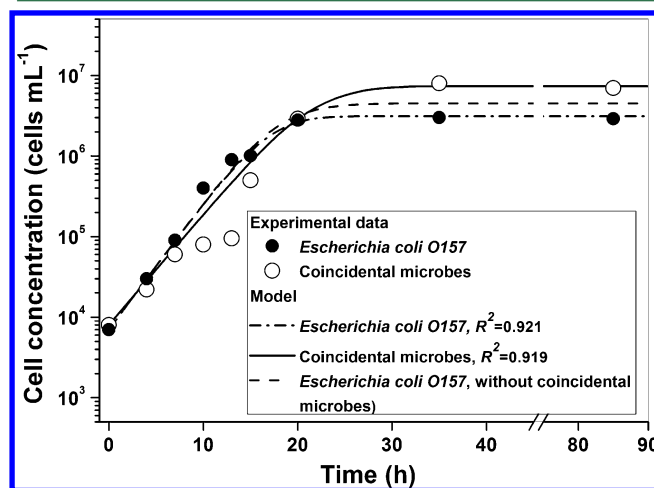

Figure 2. Observed and modeled $X_{B,Z}$) growth supported by coincidental carbon (S_{AOC}) in competition with $X_{B,BC}$: Experimental concentration of *Escherichia coli* O157 (filled circles) and coincidental microbes (open circles); simulated concentrations of *Escherichia coli* O157 (dashed-dotted line) and coincidental microbes (solid line); and simulated concentrations of *Escherichia coli* O157 without coincidental microbes (dashed line).

parameters for both *E. coli* O157 and coincidental microbes by separately growing *E. coli* O157 and coincidental microbes in the coincidental carbon environment (Scenario 1 experiments, yielding K, μ_{max} and Y). We used these parameters to simulate the competition between *E. coli* O157 and coincidental microbes (Scenario 2). The parameter values are summarized in Table 2. Correlation coefficients (R^2) between model predicted and experimental data were used to infer goodness of fit. Using the kinetic parameters inferred from the Scenario 1

experiments, the model provided good fits, for both *E. coli* (R^2 = 0.921) and coincidental microbe (R^2 = 0.919) cell numbers (solid lines in Figure 2). We also considered the growth of *E. coli* O157 on the coincidental carbon in the absence of the coincidental microbes. These data are shown as a dashed line in Figure 2. The predicted stationary phase concentration of *E. coli* O157 was 1.5 times higher than the actual concentration. Clearly, when competition between *E. coli* O157 and the coincidental microbes is considered the predicted and measured stationary phase concentrations of *E. coli* O157 and the coincidental microbes agree better. The improved prediction is significant, as bacterial concentrations in this study, were obtained by flow cytometry, which provides experimental errors as small as 5%.[16]

In their work, Vital et al. estimated that 53% of the coincidental carbon (i = 0.53) was available for *E. coli* O157 throughout the experiment.[24] In our simulations, we use this value for the available coincidental carbon $S_{AOC,Z}$ as the initial condition in our model structure and allow it to change as *E. coli* O157 competes with the coincidental microbes for $S_{AOC,Z}$, which is governed by their kinetic properties. The improved fit of the simulations to the measured data highlights the importance of this consideration.

Mixed Substrates, Single Microbe(s). Scenario 3 considers the effect of coincidental carbon on trace-level pesticide biodegradation. All environmental waters contain coincidental organic carbon of different qualities and different amounts, with ground waters often containing very low ($\sim$10 μg L^{-1})[14] and stagnant pond waters containing very high concentrations ($\sim$1000 μg L^{-1}).[38] However, of this coincidental carbon only a fraction can support microbial growth (i.e., the AOC in some reports[14,24]), and typically specific pollutant degraders can access only a fraction (i in our model) of that AOC. Here, we formalize these observations, and provide some inferences using the model framework to predict how coincidental carbon can affect the activity of pesticide degrading strains.

Using this framework, we can predict how the amount of biodegradable coincidental carbon and its accessibility to pesticide degrading strains would affect pesticide removal rates. Here we simulate batch experiments with a low initial specific degrader cell concentration ($X_{TP,0}$ 1000 cell L^{-1}), and a range of initial pesticide ($S_{TP,0}$ 10, 100, and 1000 μg L^{-1}) and coincidental carbon concentrations (S_{AOC0} from 0 to 10000 μg L^{-1}). The pesticide degrader was assumed to be able to access 0, 10, 50, or 100% of the AOC (i.e., i = 0, 0.1, 0.5, and 1).

While the calculated specific pesticide removal rates decrease as the coincidental carbon concentration increases, the specific growth rates increase (Figure 3A, B). This increase is because the pesticide degrading cells can now also grow on the coincidental carbon, and not just on the pesticide. The only exception are the situations when S_{AOC} = 0 or i = 0: under those conditions there is no coincidental carbon accessible for growth of the pesticide degrader. The main interest is however on the overall removal rate, which is the product of the specific removal rate and the concentration of pesticide degraders becasue of addditional growth on AOC the overall removal rate can only increase (Figure 3C). Clearly, positive and increasing values of R indicate that pesticide degradation rates increase with coincidental carbon concentration. Hence, with this modeling approach, we can now explain why the presence of coincidental carbon can have both neutral or positive effects on pesticide removal, as observed experimentally: as the quality in terms of overal biodegradability or accessibly to the specific
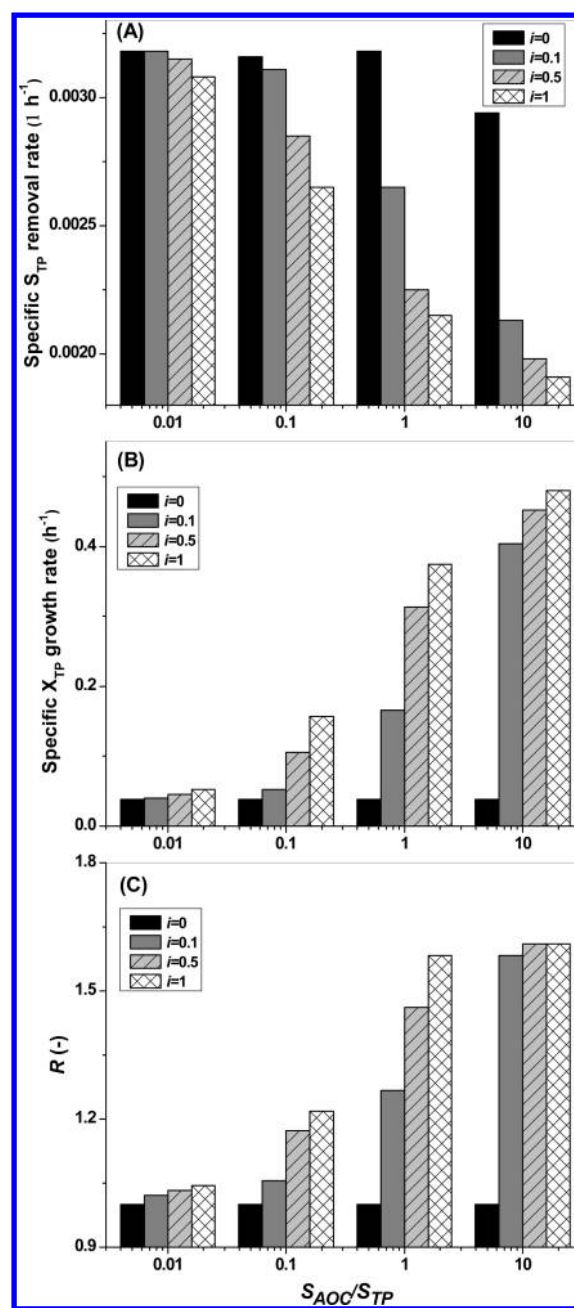

Figure 3. Effect of different initial S_{AOC} amounts (expressed as S_{AOC}/S_{TP}) and different S_{AOC} accessibilities (measured via i) on S_{TP} specific removal rate (Panel A), specific degrader X_{TP} specific growth rate (Panel B) and volumetric S_{TP} removal rate R (actual removal rate divided by removal rate in absence of S_{AOC} (i = 0)) (Panel C).

degrader increases the coincidental carbon effect becomes more positive. Our model supports the observations by Horemans et al.,[39] who reported for several specialized degrader strains that many environmental carbon sources had a positive or neutral effect on the degradation of trace-level linuron. We must, however, point out that also negative or inhibitory effects of coincidental carbon on trace pesticide degradation have been noted.[21] Such effects are currently not considered in our model framework, and would require expansion with additional biochemical details. Some of these effects may be explained by catabolite represssion (e.g., the case of citrate[39]), but the inhibition of pesticide degradation by coincidental carbon is a
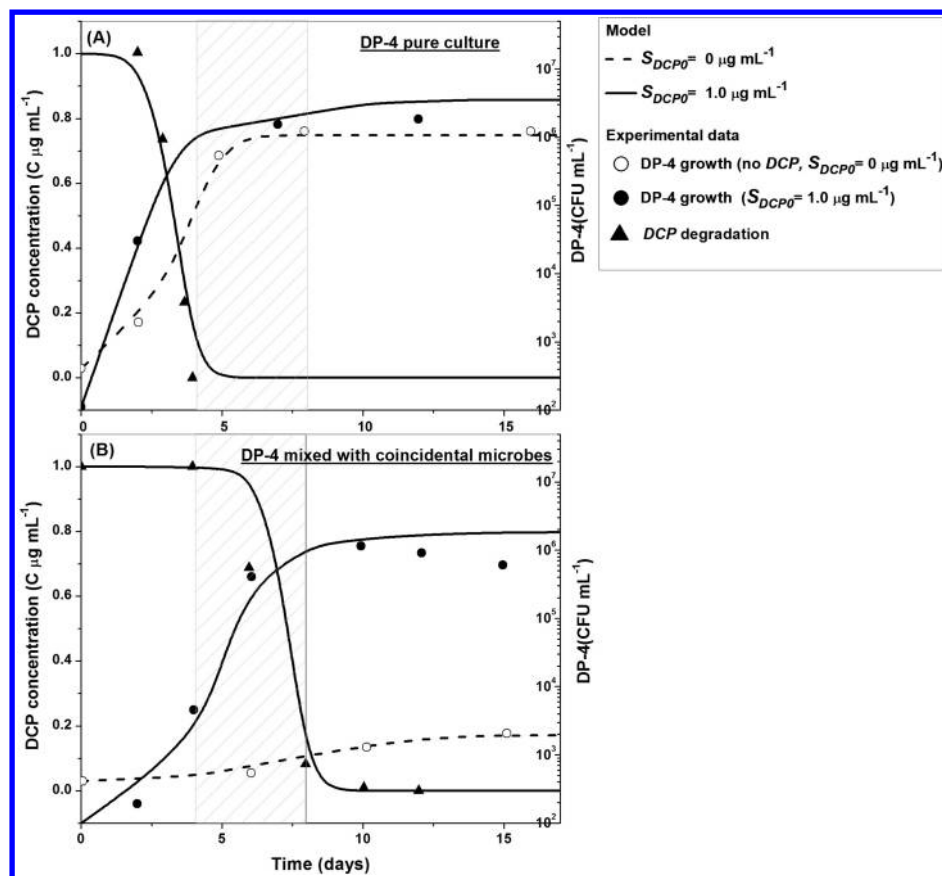
Figure 4. Observed and simulated concentrations of DCP (solely degraded by a specific degrader strain DP-4) and number of DP-4 cells in the absence (panel A) or presence (panel B) of coincidental microbes ($X_{B,BC}$) in a mineral medium containing coincidental carbon. (S_{DCP0}= 1.0 C μg mL^{-1}, solid line and solid dots; S_{DCP0}= 0 C μg mL^{-1}, dashed line and open dots).

rare phenomenon likely specific to certain AOC types and requires further study.

Mixed Substrates, Mixed Microbes. Scenario 4 considers the joint effect of coincidental carbon and coincidental microbes on trace-level pesticide biodegradation. Tarao et al.[20] examined the competition between a 2,4-dichlorophenol (DCP) degrader (DP-4) and coincidental microbes for coincidental carbon in the presence/absence of various amounts of DCP. In the absence of DCP, coincidental carbon in the mineral medium could support DP-4 growth to a density of 10^6 CFU mL^{-1}; but when coincidental microbes were added, the density of DP-4 did not increase beyond 10^3 CFU mL^{-1} during the incubation period. These phenomena could be well interpreted and predicted by our model framework. First, we estimated the parameters groups (K_s, μ_{max} and Y) for growth of DP-4 and coincidental microbes, separately, on coincidental carbon from their experiments; and parameters $K_{AOC,other,BC}$, $\mu_{XB,BC,AOCother,max}$ and $Y_{AOCother,BC}$ for the growth of coincidental microbes on $S_{AOC,other}$ were assumed based on this. Parameters (K, μ_{max} and Y) for DP-4 growth on DCP were estimated from experiments with different initial DCP concentration without coincidental microbes. Second, based on the experimental results, the initial available coincidental carbon ($S_{AOC,Z0}$) for DP-4 was set as 0.7 μg C mL^{-1} (μg carbon equivalent DCP per ml) and the parameter i was set as 0.1. This is because the coincidental microbes could grow to a density of 10^6 to 10^7 CFU mL^{-1}, but DP-4 could grow to a maximum density of 10^6 CFU mL^{-1}. Hence, DP-4 could utilize 10%−100% of the coincidental carbon in the mineral medium. All these parameter values and

initial conditions (Table 2, case 2) were then used for subsequent Scenario 4 simulations.

Then, by using the parameters we estimated from the separate scenarios, we predict the dynamics of both DCP removal and DP-4 growth in the presence (Figure 4A) or absence (Figure 4B) of the coincidental microbes ($X_{B,BC}$) in scenario 4 and compare them with the experimental data. Competition of DP-4 with coincidental microbes on coincidental carbon was described in Scenario 2. Model simulations and experimental data for the DP-4 ($X_{B,Z}$) competing with coincidental microbes ($X_{B,BC}$) in mineral medium are in good agreement (Figure 4B, dashed lines, R^2 = 0.82). Results show that DP-4 could effectively only use 0.1% of the available coincidental carbon in the presence of competing coincidental microbes. Besides, the model simulated both the pesticide (R^2 = 0.84) and specific strain dynamics with good agreement. At an initial DCP concentration of 1.0 C μg mL^{-1}, there was little difference in DCP degrader growth (solid dots and solid lines) in the presence or absence of coincidental microbes. In addition, DP-4 initially grew faster in presence versus absence of DCP. Here, the growth of DP-4 was supported by both DCP and coincidental carbon. When nearly 90% of DCP was degraded, the growth rate of DP-4 decreased. The time required for complete DCP degradation was extended by nearly 4 days in the presence of coincidental microbes (shaded in Figure 4). Hence, although DP-4 was able to grow on a fraction of the coincidental carbon, this fraction was so small in the presence of coincidental microbes, that pesticide removal was significantly retarded in the presence of the coincidental microbes.

The model framework could be used to further probe Scenario 4 by exploring the range of initial S_{AOC}, S_{TP} conditions (parameter values are provided in Table 2). From the case of Tarao et al.,[20] we infer that coincidental microbes utilize the coincidental carbon at much higher rates than the pesticide degrader (in their case, $\mu_{XB,Z,BC,AOC,max}/\mu_{XB,BC,AOCz,max} = 0.0075$, $K_{AOC,Z}/K_{AOC,Z,BC} = 0.025$). Figure 5 shows the effect of S_{AOC},
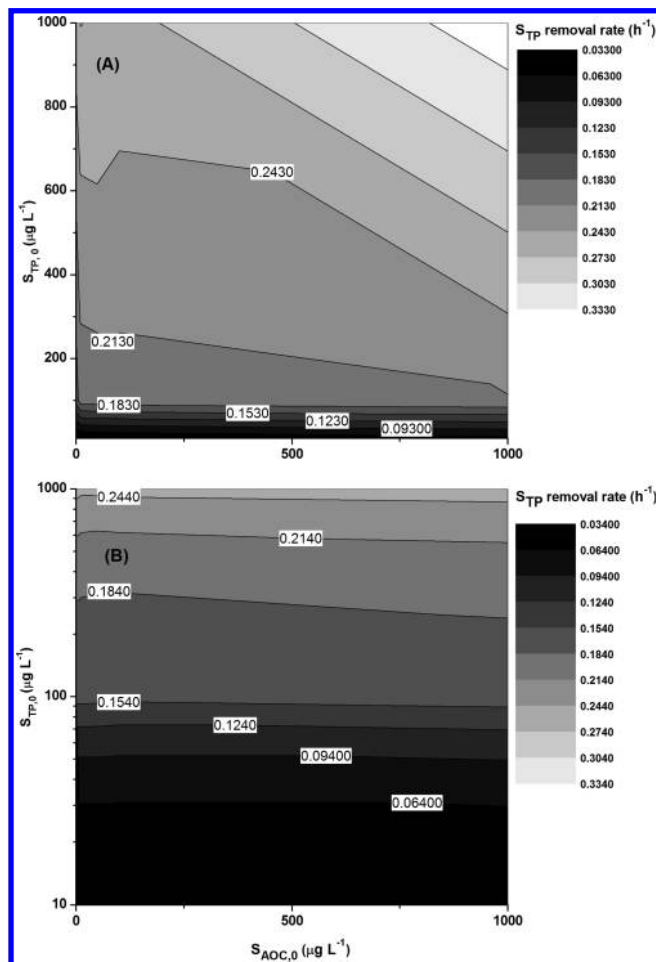

Figure 5. Effect of $X_{B,BC}$ on S_{TP} removal rate (h^{-1}) at different initial $S_{AOC, 0}$, $S_{TP, 0}$ conditions ($i = 0.5$): (A) Scenario 3, absence of $X_{B,BC}$; (B) Scenario 4, presence of $X_{B,BC}$.

$X_{B,BC}$ on the degradation rate of the pesticide at different initial $S_{AOC,0}$, $S_{TP,0}$ conditions. In the absence of $X_{B,BC}$ (Scenario 3), the S_{TP} removal rate (h^{-1}) increases with the increase of AOC concentration (Figure 5A), and the effect of AOC increases with the increase of initial pesticide concentration. In these simulations, coincidental carbon does not typically promote pesticide degradation rates when $X_{B,BC}$ is present (Scenario 4, Figure 5B). On the other hand, the positive effect of S_{AOC} on S_{TP} degradation, in the absence of $X_{B,BC}$, becomes only pronounced at elevated S_{TP} concentrations ($S_{TP} > 100 \ \mu g/L$, Figure 5A). This is because in this simulation, the maximum specific growth rate of $X_{B,Z}$ on S_{TP} is assumed much higher than on S_{AOC} ($\mu_{XB,Z,TP,max}/\mu_{XB,Z,AOC,max} = 10$).

Growth of $X_{B,Z}$ on AOC contributes to pesticide degradation, but when $X_{B,BC}$ is present, the competition for AOC reduces this advantage, even at elevated AOC concentrations. These predictions are, to a large extent, contingent on the growth kinetic advantage of coincidental microbes on the coincidental carbon. Were this condition relaxed, coincidental carbon would continue to provide an advantage to the pesticide degrader. Growth on coincidental carbon substrates has been poorly studied,[17,20,24] and requires attention, specifically to allow an estimation of stoichiometric and kinetic parameters.

Implications of This Work. Experiments that evaluate biodegradation scenarios of pollutants, including pesticides, at trace concentrations are difficult to perform. As a result, experimental data is limited. Models can help to simulate situations that are underrepresented by experimental data. Here, we developed and validated a model framework based on available experimental data to describe growth-linked biodegradation of trace-level pollutants. The model is simple and additive and assumes only kinetic effects of the interactions between the different variables. Specifically, the model considers coincidental carbon and coincidental microbes directly controlling trace pollutant degradation rates. We probed the scenarios through simulations to gain insights into process that have not been thoroughly explored experimentally (e.g., the effect of different micropollutant to AOC ratios, Figures 3 and 5). Interestingly, kinetic interactions can explain most of the published experimental data. Clearly, the quality and quantity of the coincidental carbon, as well as the presence of coincidental microbes plays a role in the kinetics of trace pollutant degradation. As a result, our model can explain phenomena that were previously unexplained or unexplored (the effect of coincidental carbon and coincidental microbes), and can be used as a tool to guide further experimental assessment of trace-level pollutant biodegradation.

■ AUTHOR INFORMATION

Corresponding Author

*Fax: +45 45 93 28 50; e-mail: bfsm@env.dtu.dk.

Notes

The authors declare no competing financial interest.

■ REFERENCES

(1) Benner, J.; Helbling, D. E.; Kohler, H. P. E.; Wittebol, J.; Kaiser, E.; Prasse, C.; Ternes, T. A.; Albers, C. N.; Aamand, J.; Horemans, B.; Springael, D.; Walravens, E.; Boon, N. Is biological treatment a viable alternative for micropollutant removal in drinking water treatment processes? *Water Res.* **2013**, *47* (16), 5955−5976.

(2) Huntscha, S.; Singer, H.; Canonica, S.; Schwarzenbach, R. P.; Fenner, K. Input dynamics and fate in surface water of the herbicide metolachlor and of its highly mobile transformation product metolachlor ESA. *Environ. Sci. Technol.* **2008**, *42* (15), 5507−5513.

(3) Fenner, K.; Canonica, S.; Wackett, L. P.; Elsner, M. Evaluating Pesticide Degradation in the Environment: Blind Spots and Emerging Opportunities. *Science.* **2013**, *341* (6147), 752−758.

(4) Alexander, M. Biodegradation of chemicals of environmental concern. *Science.* **1981**, *211* (4478), 132−138.

(5) Albers, C. N.; Jacobsen, O. S.; Aamand, J. Using 2,6-dichlorobenzamide (BAM) degrading Aminobacter sp MSH1 in flow through biofilters-initial adhesion and BAM degradation potentials. *Appl. Microbiol. Biot.* **2014**, *98* (2), 957−967.

(6) McDowall, B.; Hoefel, D.; Newcombe, G.; Saint, C. P.; Ho, L. Enhancing the biofiltration of geosmin by seeding sand filter columns with a consortium of geosmin-degrading bacteria. *Water Res.* **2009**, *43* (2), 433−440.

(7) Lewis, D. L.; Hodson, R. E.; Freeman, L. F. Multiphasic kinetics for transformation of methyl parathion by flavobacterium species. *Appl. Environ. Microb.* **1985**, *50* (3), 553−557.

(8) Rapp, P. Multiphasic kinetics of transformation of 1,2,4-trichlorobenzene at nano- and micromolar concentrations by Burkholderia sp strain PS14. *Appl. Environ. Microbiol.* **2001**, *67* (8), 3496−3500.

(9) Torang, L.; Nyholm, N.; Albrechtsen, H. J. Shifts in biodegradation kinetics of the herbicides MCPP and 2,4-D at low concentrations in aerobic aquifer materials. *Environ. Sci. Technol.* **2003**, *37* (14), 3095−3103.

(10) Tros, M. E.; Schraa, G.; Zehnder, A. J. B. Transformation of low concentrations of 3-chlorobenzoate by Pseudomonas sp strain B13: Kinetics and residual concentrations. *Appl. Environ. Microbiol.* **1996**, *62* (2), 437−442.

(11) Helbling, D. E.; Hammes, F.; Egli, T.; Kohler, H. P. Kinetics and yields of pesticide biodegradation at low substrate concentrations and under conditions restricting assimilable organic carbon. *Appl. Environ. Microbiol.* **2014**, *80* (4), 1306−13.

(12) Kovarova-Kovar, K.; Egli, T. Growth kinetics of suspended microbial cells: From single-substrate-controlled growth to mixed-substrate kinetics. *Microbiol. Mol. Biol. Rev.* **1998**, *62* (3), 646−666.

(13) Grady, C. P. L.; Smets, B. F.; Barbeau, D. S. Variability in kinetic parameter estimates: A review of possible causes and a proposed terminology. *Water Res.* **1996**, *30* (3), 742−748.

(14) Egli, T. How to live at very low substrate concentration. *Water Res.* **2010**, *44* (17), 4826−4837.

(15) Escobar, I. C.; Randall, A. A.; Taylor, J. S. Bacterial growth in distribution systems: Effect of assimilable organic carbon and biodegradable dissolved organic carbon. *Environ. Sci. Technol.* **2001**, *35* (17), 3442−3447.

(16) Hammes, F. A.; Egli, T. New method for assimilable organic carbon determination using flow-cytometric enumeration and a natural microbial consortium as inoculum. *Environ. Sci. Technol.* **2005**, *39* (9), 3289−3294.

(17) Horemans, B.; Vandermaesen, J.; Smolders, E.; Springael, D. Cooperative dissolved organic carbon assimilation by a linuron-degrading bacterial consortium. *FEMS Microbiol. Ecol.* **2013**, *84* (1), 35−46.

(18) Vanderkooij, D.; Visser, A.; Hijnen, W. A. M. Determining the concentration of easily assimilable organic-carbon in drinking-water. *J. Am. Water Works Assoc..* **1982**, *74* (10), 540−545.

(19) Simkins, S.; Alexander, M. Nonlinear estimation of the parameters of monod kinetics that best describe mineralization of several substrate concentrations by dissimilar bacterial densities. *Appl. Environ. Microbiol.* **1985**, *50* (4), 816−824.

(20) Tarao, M.; Seto, M. Estimation of the yield coefficient of Pseudomonas sp strain DP-4 with a low substrate (2,4-dichlorophenol [DCP]) concentration in a mineral medium from which uncharacterized organic compounds were eliminated by a non-DCP-degrading organism. *Appl. Environ. Microbiol.* **2000**, *66* (2), 566−570.

(21) Rentz, J. A.; Alvarez, P. J. J.; Schnoor, J. L. Repression of Pseudomonas putida phenanthrene-degrading activity by plant root extracts and exudates. *Environ. Microbiol.* **2004**, *6* (6), 574−583.

(22) Horemans, B.; Hofkens, J.; Smolders, E.; Springael, D. Biofilm formation of a bacterial consortium on linuron at micropollutant concentrations in continuous flow chambers and the impact of dissolved organic matter. *FEMS Microbiol Ecol.* **2014**, *88* (1), 184−94.

(23) Tan, D. T.; Arnold, W. A.; Novak, P. J. Impact of organic carbon on the biodegradation of estrone in mixed culture systems. *Environ. Sci. Technol.* **2013**, *47* (21), 12359−12365.

(24) Vital, M.; Hammes, F.; Egli, T. Competition of *Escherichia coli* O157 with a drinking water bacterial community at low nutrient concentrations. *Water Res.* **2012**, *46* (19), 6279−6290.

(25) Van Nevel, S.; De Roy, K.; Boon, N. Bacterial invasion potential in water is determined by nutrient availability and the indigenous community. *FEMS Microbiol Ecol.* **2013**, *85* (3), 593−603.

(26) Dejonghe, W.; Berteloot, E.; Goris, J.; Boon, N.; Crul, K.; Maertens, S.; Hofte, M.; De Vos, P.; Verstraete, W.; Top, E. M.

(27) Sorensen, S. R.; Ronen, Z.; Aamand, J. Growth in coculture stimulates metabolism of the phenylurea herbicide isoproturon by Sphingomonas sp strain SRS2. *Appl. Environ. Microbiol.* **2002**, *68* (7), 3478−3485.

(28) Jones, S. H.; Alexander, M. Kinetics of mineralization of phenols in lake water. *Appl. Environ. Microbiol.* **1986**, *51* (5), 891−897.

(29) Fuchslin, H. P.; Schneider, C.; Egli, T. In glucose-limited continuous culture the minimum substrate concentration for growth, s(min), is crucial in the competition between the enterobacterium *Escherichia coli* and *Chelatobacter heintzii*, an environmentally abundant bacterium. *ISME J.* **2012**, *6* (4), 777−789.

(30) Henze, M.; Sutton, P. M.; Gujer, W.; Koller, J.; Grau, P.; Elmaleh, S.; Grady, C. P. L. The use and abuse of notation in biological wastewater treatment. *Water Res.* **1982**, *16* (6), 755−757.

(31) Corominas, L.; Rieger, L.; Takacs, I.; Ekama, G.; Hauduc, H.; Vanrolleghem, P. A.; Oehmen, A.; Gernaey, K. V.; van Loosdrecht, M. C. M.; Comeau, Y. New framework for standardized notation in wastewater treatment modelling. *Water Sci. Technol.* **2010**, *61* (4), 841−857.

(32) Adam, I. K. U.; Rein, A.; Miltner, A.; Fulgencio, A. C. D.; Trapp, S.; Kastner, M. Experimental results and integrated modeling of bacterial growth on an insoluble hydrophobic substrate (phenanthrene). *Environ. Sci. Technol.* **2014**, *48* (15), 8717−8726.

(33) Bosma, T. N. P.; Middeldorp, P. J. M.; Schraa, G.; Zehnder, A. J. B. Mass transfer limitation of biotransformation: Quantifying bioavailability. *Environ. Sci. Technol.* **1997**, *31* (1), 248−252.

(34) Ihssen, J.; Egli, T. Global physiological analysis of carbon- and energy-limited growing Escherichia coli confirms a high degree of catabolic flexibility and preparedness for mixed substrate utilization. *Environ. Microbiol.* **2005**, *7* (10), 1568−1581.

(35) McFall, S. M.; Abraham, B.; Narsolis, C. G.; Chakrabarty, A. M. A tricarboxylic acid cycle intermediate regulating transcription of a chloroaromatic biodegradative pathway: Fumarate-mediated repression of the clcABD operon. *J. Bacteriol.* **1997**, *179* (21), 6729−6735.

(36) Simonsen, A.; Badawi, N.; Anskjaer, G. G.; Albers, C. N.; Sorensen, S. R.; Sorensen, J.; Aamand, J. Intermediate accumulation of metabolites results in a bottleneck for mineralisation of the herbicide metabolite 2,6-dichlorobenzamide (BAM) by Aminobacter spp. *Appl. Microbiol. Biot.* **2012**, *94* (1), 237−245.

(37) Sorensen, S. R.; Rasmussen, J.; Jacobsen, C. S.; Jacobsen, O. S.; Juhler, R. K.; Aamand, J. Elucidating the key member of a linuron-mineralizing bacterial community by PCR and reverse transcription-PCR denaturing gradient gel electrophoresis 16S rRNA gene fingerprinting and cultivation. *Appl. Environ. Microb.* **2005**, *71* (7), 4144−4148.

(38) Vital, M.; Hammes, F.; Egli, T. Escherichia coli O157 can grow in natural freshwater at low carbon concentrations. *Environ. Microbiol.* **2008**, *10* (9), 2387−2396.

(39) Horemans, B.; Vandermaesen, J.; Vanhaecke, L.; Smolders, E.; Springael, D. Variovorax sp.-mediated biodegradation of the phenyl urea herbicide linuron at micropollutant concentrations and effects of natural dissolved organic matter as supplementary carbon source. *Appl. Microbiol. Biotechnol.* **2013**, *97* (22), 9837−9846.

Synergistic degradation of linuron by a bacterial consortium and isolation of a single linuron-degrading Variovorax strain. *Appl. Environ. Microbiol.* **2003**, *69* (3), 1532−1541.